Available online at www.sciencedirect.com
ScienceDirect
Trans. Nonferrous Met. Soc. China 28(2018) 866−878
Transactions of Nonferrous Metals Society of China
www.tnmsc.cn

Microstructure and wear performance of Al5083/CeO_2/SiC mono and hybrid surface composites fabricated by friction stir processing

M. AMRA, Khalil RANJBAR, S. A. HOSSEINI

Department of Materials Science and Engineering, Faculty of Engineering, Shahid Chamran University of Ahvaz, Ahvaz 61357, Iran

Received 20 February 2017; accepted 29 September 2017

Abstract: Friction stir processing (FSP) was utilized to produce surface composites by incorporating nano-sized cerium oxide (CeO_2) and silicon carbide (SiC) particles individually and in combined form into the Al5083 alloy matrix. The study signified the role of these reinforcements on microstructure and wear behavior of the resultant surface composite layers. The wear characteristics of the resultant mono and hybrid surface composite layers were investigated using a pin-on-disc wear tester at room temperature. The microstructural observations of FSPed regions and the worn out surfaces were performed by optical and scanning electron microscopy. Considerable grain refinement and uniform distribution of reinforcement particles were achieved inside the nugget zone. All the composite samples showed higher hardness and wear resistance compared to the base metal. Among the composite samples, the hybrid composite (Al5083/CeO_2/SiC) revealed the highest wear resistance and the lowest friction coefficient, whereas the Al5083/SiC composite exhibited the highest hardness, i.e., 1.5 times as hard as that of the Al5083 base metal. The enhancement in wear behavior of the hybrid composites was attributed to the solid lubrication effect provided by CeO_2 particles. The predominant wear mechanism was identified as severe adhesive in non-composite samples, which changed to abrasive wear and delamination in the presence of reinforcing particles.

Key words: Al5083 alloy; friction stir processing; CeO_2; SiC; surface composites; wear mechanism

1 Introduction

Aluminum metal matrix composites (AMMCs) have attracted much attention in aerospace and automotive industries due to their low density, higher specific strength and noticeable wear resistance [1]. Nonetheless, AMMCs show low ductility and toughness due to the presence of hard and non-deformable ceramic reinforcement particles. With fabrication of a metal matrix composite layer on the surface of metal (called surface metal matrix composites — SMMCs), it is possible to utilize combination of high tribological properties of the surface layer and high toughness of the interior bulk metal [2]. Several techniques such as powder metallurgy [2], cast sintering [3], electron beam irradiation [4], plasma spraying [5], and high energy laser melt injection [6], have been adopted to fabricate SMMCs. In most cases, the high processing temperature causes the interfacial reaction between reinforcement and metal matrix and the formation of detrimental phases. By treating SMMCs based on solid state processing techniques, the problems mentioned above can be eliminated.

A simple, economic and solid state process for the fabrication of SMMCs, is friction stir processing (FSP) which is based on the principles of friction stir welding (FSW) [7−17]. The basic concept of FSP is remarkably simple. The reinforcement particles are introduced in pre-machined grooves/holes on the surface of the metallic substrate plate. Then, a non-consumable rotating tool with a specially designed pin and a shoulder is plunged inside a desired path on the surface of the substrate. The frictional heating and sever plastic deformation imposed by the rotating tool promotes intermixing of particles and the substrate in the near surface layer of the processed metallic substrate [18]. Reinforcing particles could be in mono or hybrid form. Hybrid aluminum matrix surface composites with a mixture of two or more different types of particles have been described to show better properties in comparison with the mono particle composites [9−17]. Indeed, in

Corresponding author: Khalil RANJBAR; Tel/Fax: +98-6133336642; E-mail: k_ranjbar@scu.ac.ir
DOI: 10.1016/S1003-6326(18)64720-X

order to achieve the mutual advantages of different types and/or forms of reinforcement particles, a combined mixture of these particles is preferred.

SOLEYMANI et al [9] studied the tribological behavior of the surface mono and hybrid composites of Al5083/SiC/MoS_2. In hybrid composite, MoS_2 particles formed a solid lubricating film and the highest wear resistance was obtained. MOSTAFAPOUR-ASL and KHANDANI [10] evaluated the effect of the hybrid ratio on mechanical, microstructural and wear properties of surface hybrid nano-composites of Al5083/graphite/Al_2O_3 fabricated by FSP. They reported that hybrid ratio is a key factor and a better combination of wear and tensile properties resulted in graphite hybrid ratio of 50%. MAHMOUD-ESSAM et al [11] utilized FSP to produce Al1050/SiC/Al_2O_3 mono and hybrid SMMCs and evaluated the wear characteristics of the resultant composites. They reported that the wear behavior of the composites is dependent upon applied load and the mass ratio of SiC to Al_2O_3. MAXWELL-REJIL et al [12] reported a successful fabrication of Al6360/TiC/B_4C hybrid SMMCs via FSP. In their study, the addition of TiC and B_4C particles enhanced the wear resistance of Al6360 and, Al6360/50%TiC+50%B_4C hybrid SMMC offered the lowest wear rate due to the formation of a thin tribo-film. YUVARAJ et al [13] incorporated nano-particles of B_4C and TiC into the matrix of Al5083 alloy individually and in combined form in order to produce mono and hybrid surface composite layers, and significant improvement in wear resistance was obtained in hybrid composite.

The aim of the present study was to produce Al5083/CeO_2/SiC mono and hybrid composite layers by FSP technique on Al5083 alloy substrate and, to investigate the effect of these reinforcements on the microstructure and wear behavior of the resultant surface composite layers. Silicon carbide (SiC) powder was widely used to reinforce aluminum alloys because of its low density and high hardness [8,9,11,15,17,19], and cerium oxide (CeO_2) was another potential reinforcement particle which had good adhesion and high stability against mechanical abrasion and high temperature and cathodic inhibitor property [20−23]. The effect of incorporating CeO_2 reinforcing particles (either individuality or in combination with other reinforcing particles such as SiC) on wear performance of Al5083 has not been reported so far.

2 Experimental

In the present study, an Al5083 rolled plate was used as the base metal. Its chemical composition is given in Table 1. Samples with dimensions of 5 mm × 100 mm × 250 mm were cut from the base metal and used for the FSP.

Table 1 Chemical composition of Al5083 alloy (mass fraction, %)

Mg	Mn	Fe	Cr	Si	Ti	Cu	Zn	Al
4.51	0.4	0.4	0.11	0.22	0.04	0.06	0.06	Bal.

Two nano-sized ceramic particles of CeO_2 (~50 nm) and SiC (~80 nm) supplied by the Neotrino Co., Tehran, were used as reinforcements. The scanning electron microscope (SEM) images of these reinforcements are shown in Fig. 1. The fabricated surface composites were noted as Al5083/CeO_2, and Al5083/SiC mono composites and the hybrid composite Al5083/CeO_2/SiC. A sample which was subjected to FSP with no reinforcement was named as FSPed base metal.

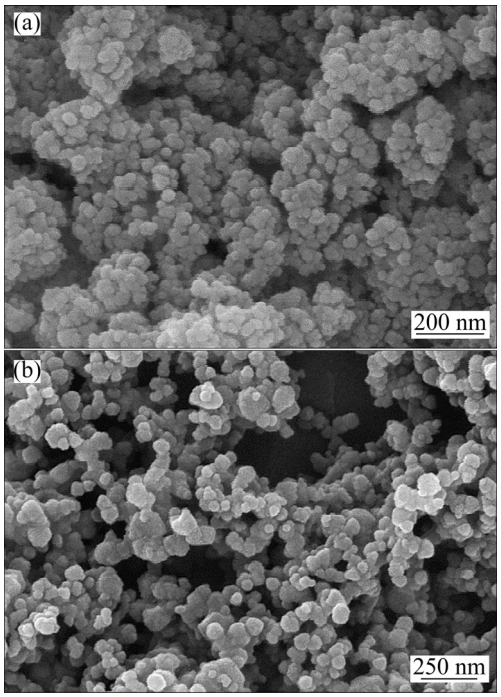

Fig. 1 SEM images of CeO_2 (a) and SiC (b) reinforcement particles

Figure 2 shows the schematic view and image of the FSP setup and tool. A hot worked tool steel H13 with a concave shoulder of 18 mm in diameter and a threaded cylindrical pin of 6 mm in diameter and 4.5 mm in height was used to perform the FSP. The reinforcement particles were packed in a longitudinal groove with 1.2 mm in width, 2 mm in depth and 230 mm in length, machined on the surface of the Al5083 plates. Therefore, all samples had constant volume fraction of reinforcement. A pinless tool was initially employed to close the filled grooves to prevent powder from splashing during the process. Then, a tool with a pin and a shoulder were

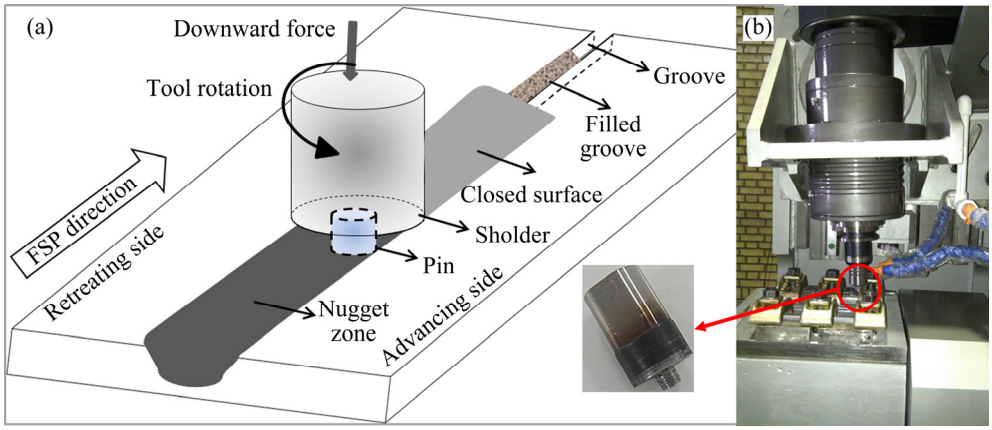

Fig. 2 Schematic illustration of FSP setup and its elements (a) and actual FSP machine and FSP tool used in this study (b)

plunged into the plate and traveled along the closed groove. Three passes of FSP were used for homogeneous dispersion of reinforcement. The first two passes were performed at a rotational speed of 800 r/min and a traveling speed of 35 mm/min, whereas the third pass was done at a rotational speed of 600 r/min and a traveling speed of 45 mm/min. For all the passes, a tool tilt angle of 3° was maintained throughout the process. In the second pass, the tool was travelled along the same line as the first and third ones but in the opposite direction. In other words, the advancing side of the first and third passes became the retreating side in the second pass and vice versa.

Microstructural observations were performed by ΣIGMA/VP-ZESIS optical microscope (OM) and VEGA-TSCAN SEM equipped with an energy dispersive X-ray spectroscopy (EDS) on the cross section of processed samples.

The average of three sets of micro-hardness values along the cross section at different distances from top surface of FSPed samples was determined by a micro-hardness test using a Vickers indenter at a load of 200 g and a dwell time of 15 s.

The sliding wear behavior of the FSPed samples and base metal was measured using a pin-on-disc wear test machine (Manual tribometer: Type TRM250, WAZAU, Germany) at room temperature against the counterface of a hardened disk of E52100 (100Cr6) steel with hardness of HRC 62−65. Cylindrical pin specimens with 8 mm in diameter and 4.7 mm in thickness were prepared from the center of the nugget zone (NZ) by machining. The axis of the pins was perpendicular to the tool travel direction. The wear test was conducted at a sliding velocity of 0.24 m/s, a normal force of 24 N and a sliding distance of 1 km. Friction coefficient and pin height loss at different sliding distances were automatically measured by the wear test machine. For this purpose, a computer aided data acquisition system was used. The wear volume loss was calculated by multiplying the cross sectional area of the test pin by its loss of height. The wear rate was obtained by dividing wear volume loss to sliding distance. Each test was repeated three times with identical new samples on fresh disk surface track, and average of data was used to compute wear volume loss and wear rate. The worn surfaces of wear test specimens were observed using SEM without removing the surficial debris. The wear debris was collected and characterized using SEM.

3 Results and discussion

3.1 Microstructure

The modification in grain structure and the distribution of primary intermetallic particles in Al5083 alloy before and after FSP are presented in Fig. 3. It can be seen that due to the severe plastic deformation, mechanical mixing, and frictional heating generated during FSP, the initial rolled grain size of the base metal (Fig. 3(a)) was considerably reduced and transformed to a more homogeneous and equiaxed one after the application of FSP (Fig. 3(b)). This clear grain structure modification and its refinement are attributed to dynamic recrystallization phenomenon which occurs in FSP [24,25]. Due to FSP, the larger primary intermetallic particles (Fig. 3(c)) also fragmented to smaller ones and redistributed throughout the matrix (Fig. 3(d)) more uniformly. Figure 3(e) shows the EDS spectrum of these intermetallic particles which were mainly composed of Al, Mn, and Fe elements and expected to be $Al_6(Fe,Mn)$ compound. It is reported that these particles did not dissolve in NZ [26], instead they acted as recrystallization sites through particle-simulated nucleation (PSN) mechanism [27,28].

Figure 4 shows the effect of number of FSP passes on the homogeneity of the microstructure in the NZ for the hybrid SMMC. Usually, different microstructural

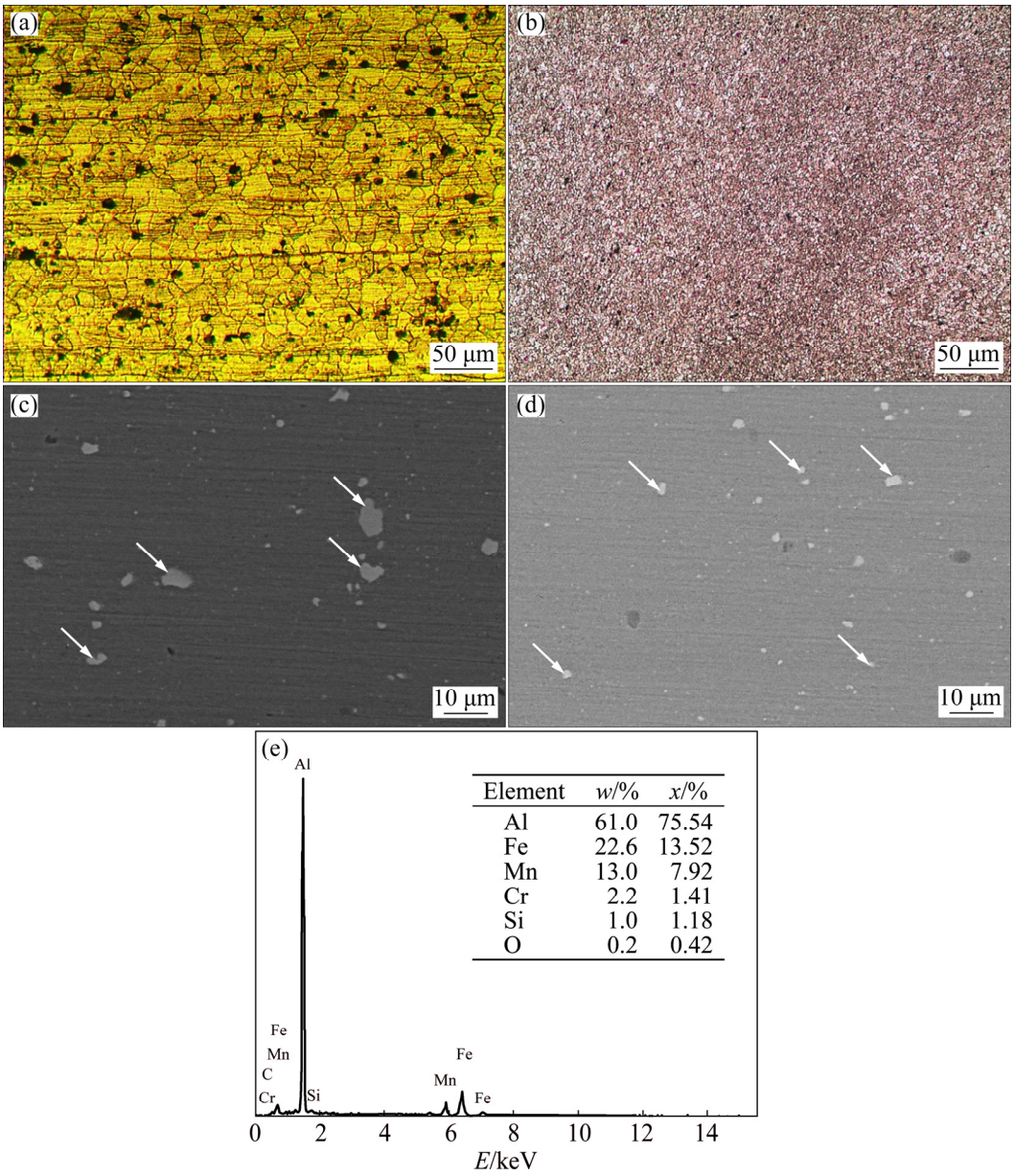

Fig. 3 OM images of Al5083 base alloy before (a) and after (b) applying FSP, SEM images displaying in distribution of primary intermetallic particles in base alloy before (d) and after (c) applying FSP and EDS spectrum of primary intermetallic particles (marked by white arrows) corresponding to $Al_6(Fe,Mn)$ phase compound fragmented and redistributed after subjecting to FSP (e)

features in FSP appear and they are known as onion rings/banding patterns. For an intensive material stirring in the NZ, these rings are very close together and no island (unmixed zone or grain) is formed between them [29,30]. The combination of tool rotation and traverse movement creates an asymmetric material flow and more stirring takes place on advancing side [19]. Therefore, it can be expected that increasing the number of passes and also changes in processing directions lead to a more homogeneous NZ and better distribution of reinforcements with fine grains. In the first pass (Figs. 4(a) and (b)), there are unmixed grains subjected to FSP but not properly mixed with reinforcements.

In the second pass (Fig. 4(c)), these features are eliminated and rings seem more uniform. Finally, in third pass (Fig. 4(d)), the onion rings are so intimately placed that they do not reveal clear ring or banding. Figure 4(d), also reveals sound bonding between the NZ of the hybrid SMMC and the Al5083 matrix. No particular defects such as voids or tunneling could be detected. Moreover, this figure shows that matrix grains are further refined in the presence of reinforcements.

It is reported that reinforcements can restrict grain growth of the matrix by peening effect after dynamic recrystallization and also act as nucleation sites for aluminum grains [31,32], leading to finer grains. In the

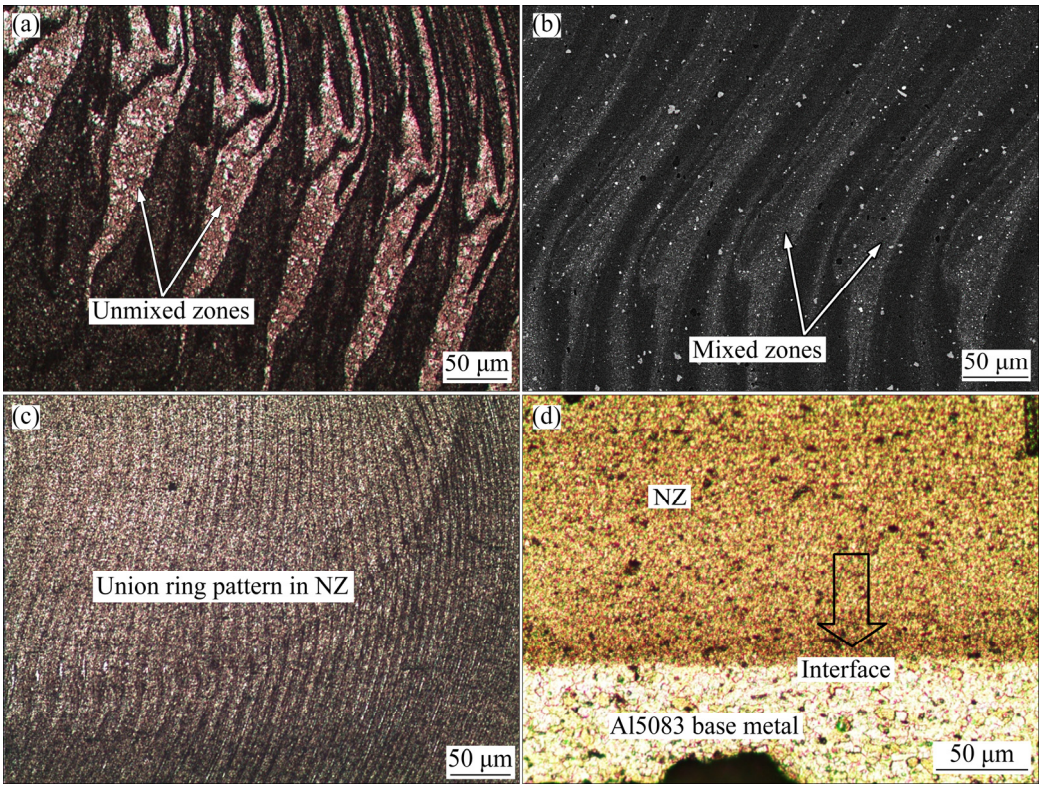

Fig. 4 Micrographs revealing effect of number of passes on homogeneity of microstructure in NZ for hybrid SMMC: (a) OM image after one pass; (b) SEM image after one pass; (c, d) OM images after two and three passes showing homogenous microstructure and sound bounding at interface between Al5083 alloy substrate and hybrid SMMC, respectively

present study, nano-size reinforcement particles (CeO_2, CeO_2+SiC, SiC), are expected to act in the same way, since they are well distributed throughout the NZ due to strong action of stirring (after three passes). The SEM images of the synthesized SMMCs and their corresponding EDS spectra are presented in Fig. 5.

In the region next to the NZ (Fig. 6), grains are distorted and stretched out in an upward flowing pattern about the rotating tool axis, identified as the thermo mechanically affected zone (TMAZ). Here, grains are partly refined and redistributed compared to those in the NZ. It is believed that, deformation strain and frictional heating in the TMAZ are not sufficient to cause perfect recrystallization [18,25].

3.2 Wear behavior

Surface hardness is an important parameter in both applied and research aspects of tribology [33]. Therefore, while considering the hardness values of the specimens, a deeper focus was made on variations of the friction coefficient, SEM images of the worn surfaces, and the morphology of their wear debris, in order to assess wear behavior and identify the dominant wear mechanisms. The variation in micro-hardness values of the nugget zone after three passes for the base metal and the other FSPed specimens is depicted in Fig. 7. The average hardness of the base metal was HV 77. For the FSPed base metal, the average hardness value was increased and reached a maximum of HV 85. This relative increase in hardness value of the FSPed specimen is expected to be due to the grain refinement and also due to the fragmentation and redistribution of primary $Al_6(Fe,Mn)$ intermetallic particles. These particles are incoherent to the matrix, which may also improve the hardness and the strength of the alloy through Orowan strengthening mechanism [34]. In the NZ, annealing effect of the FSP can reduce the micro-hardness by decreasing the density of the dislocations and residual compressive stress of initially rolled base metal. In the present study, it seems that the effect of grain refinement via dynamic recrystallization and fragmentation/redistribution of intermetallic particles compensates the annealing effect. For the FSPed composites, the average hardness values were higher.

The existence of the CeO_2 and SiC dispersed hard particles admixed with the microstructural modifications induced by the FSP could be responsible for the increase in hardness values. So, the relevant hardness increment mechanisms in this study can be summarized as follows. Firstly, according to the Hall−Petch relationship, the

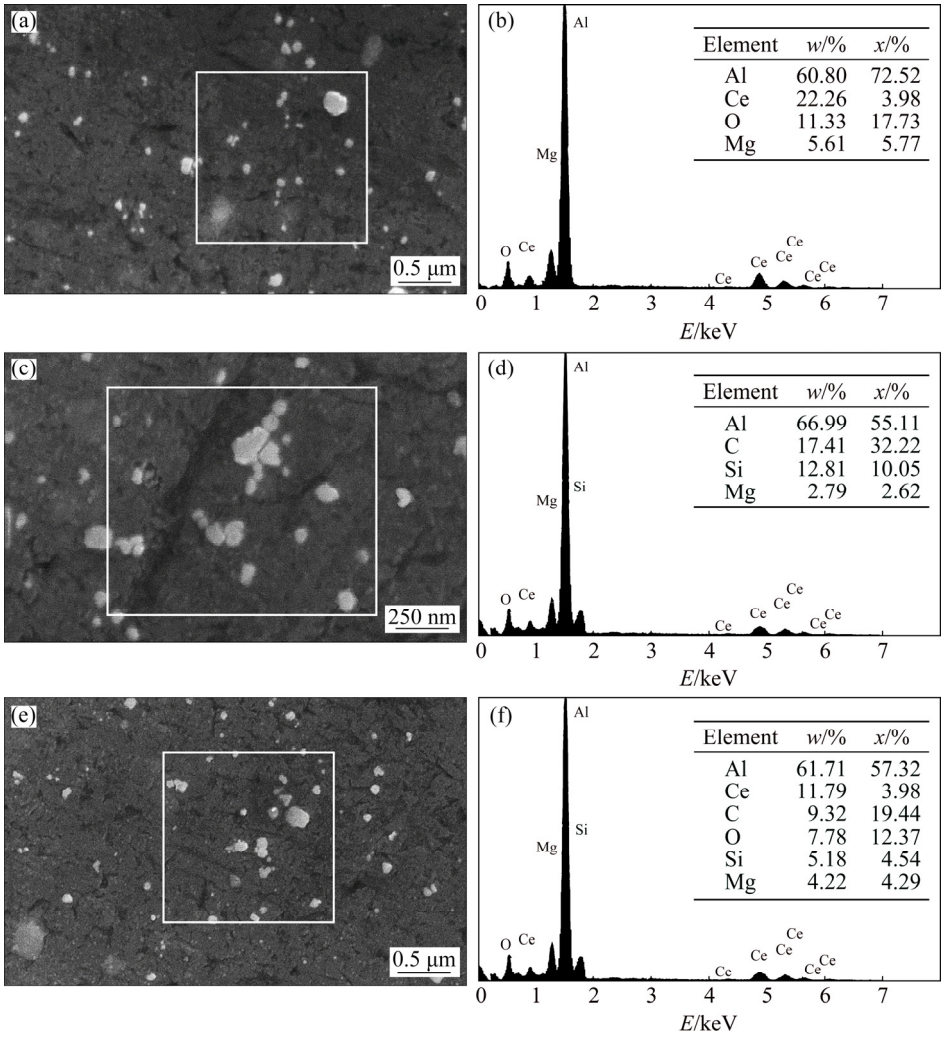

Fig. 5 SEM images showing distribution of reinforcement particles in NZ of different FSPed composites and their corresponding EDS spectra taken from regions marked by white rectangles: (a, b) Al5083/CeO_2; (c, d) Al5083/SiC; (e, f) Al5083/CeO_2/SiC hybrid composites

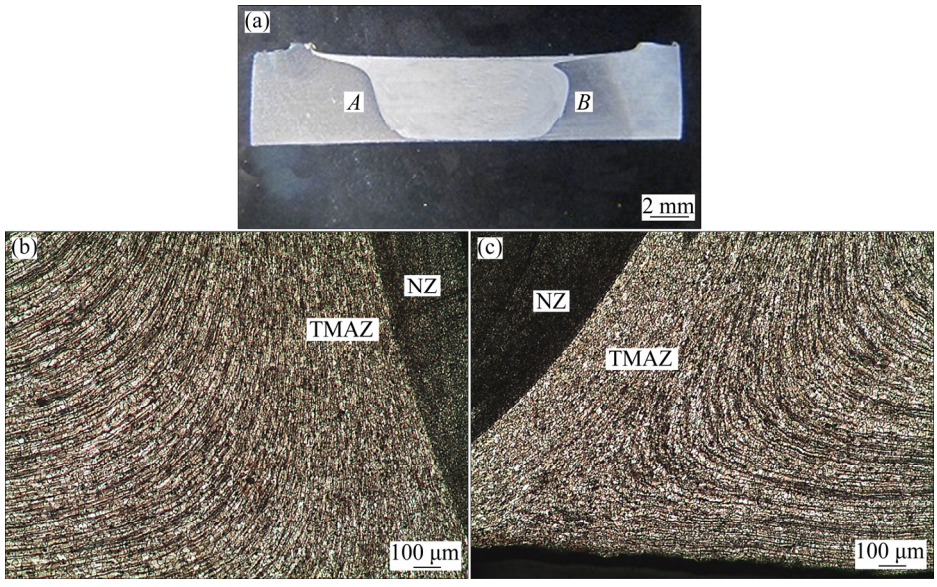

Fig. 6 Optical macrograph and micrographs of hybrid SMMC after applying three passes of FSP: (a) Macrograph of NZ; (b) Micrograph of point *A* (advancing side for the first and third passes); (c) Micrograph of point *B* (advancing side for the second pass)

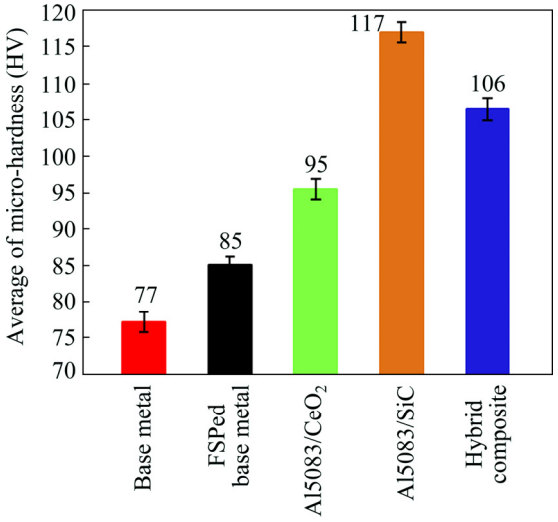

Fig. 7 Micro-hardness values for Al5083 base alloy and FSPed specimens

hardness value in the NZ is enhanced because of the grain size refinement [35]. Secondly, Orowan strengthening due to the dispersion of nano-size and non-shearable ceramic particles acts to obstruct dislocation movement [31,36] and prevents plastic deformation. Thirdly, mechanism is the pinning effect imposed on grains by homogeneous distribution of reinforcing particles and intermetallic compounds retarding the grain growth. Other mechanisms contributing partly to hardness increment include the large coefficient of thermal expansion mismatch between the Al5083 matrix and the reinforcements (quench hardening), which results in the increase and punching of dislocations at the interface, leading to work hardening of the matrix [12]. The intermetallic compounds were also fragmented and redistributed in matrix during the FSP and partly contributing to strengthening.

The increase in hardness values was evidently higher in composites reinforced with SiC and CeO_2 particles either individually or in hybrid form. The hardness values showed a sharp increase with the addition of SiC reinforcement particles, and reached a maximum value of HV 117 in the NZ for the Al5083/SiC mono composite, i.e., 1.5 times as hard as that of the Al5083 base metal. It can be due to higher hardness of SiC particles compared with CeO_2 particles, and also, larger coefficient of thermal expansion mismatch between the aluminum matrix and SiC particles relative to the aluminum matrix and CeO_2 particles.

Wear is the surface damage or removal of material from one or both of two solid surfaces in contact which are in relative motion with each other. Wear can be characterized in terms of the wear loss based on either mass change or dimensional change [33]. Figure 8 shows the variations in the measured wear volume loss versus sliding distance for the Al5083 base metal and the FSPed samples. As this figure shows, the wear volume loss increases with the increase of sliding distance and the extent of volume loss is considerably lower in the FSPed samples as compared to that of the Al5083 base metal. Furthermore, all SMMCs show lower wear volume loss compared to FSPed base metal due to the presence of reinforcement particles.

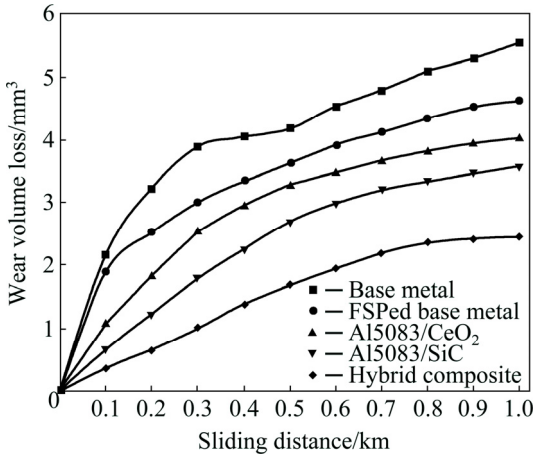

Fig. 8 Wear volume loss of Al5083 base metal and FSPed specimens as function of sliding distance

Similarly, wear behavior of different samples in terms of wear rate is presented in Fig. 9. The wear rates of the Al5083 base metal and the FSPed base metal are higher during the initial period of sliding, unlike the wear rate of SMMCs which exhibit significantly lower and steady state wear rate.

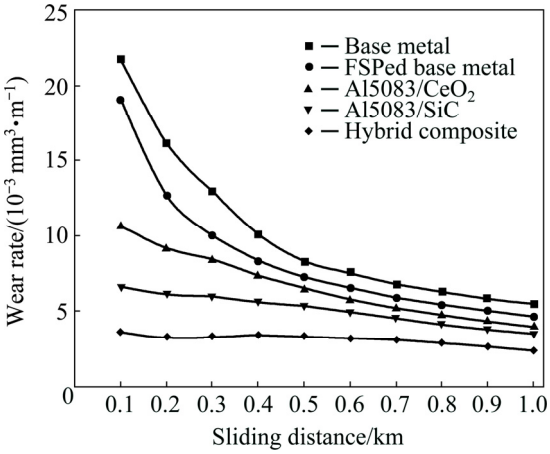

Fig. 9 Wear rates of Al5083 base metal and FSPed specimens as function of sliding distance

The minimum wear volume loss and wear rate were obtained for the FSPed hybrid composite. Comparison of Figs. 7−9 clearly shows that, the hardness values and the wear resistance (low wear volume loss and low wear

rate) are closely related to each other, i.e., specimen with higher hardness possesses higher wear resistance, except for the Al5083/SiC mono composite that exhibited the highest hardness and second best wear resistance.

The variation of friction coefficient with sliding distance is presented in Fig. 10. The typical SEM images of the worn surfaces and the wear debris are displayed in Figs. 11 and 12, respectively. In general, at the beginning of wear test, for all the tested samples, the coefficient of friction increases to a peak value, and then slows down to a steady state. The initial increased coefficient of friction is attributed to the increase in the frictional force needed to overcome the highly adhesive surface contact between the disk and the pin samples [37−39]. The periodical accumulation and elimination of wear debris on the wear track cause sudden oscillation of the friction coefficient [37] as they are observed for all samples in Fig. 10. The banding structure and formation of surface pits during sliding also lead to such oscillation due to disk–pin surface mismatch [7,18]. The mean friction coefficient value of the Al5083 base metal was found to be ~0.66 against ~0.57 of FSPed base metal. This is true because in the latter case metal surface is harder and shows lower tendency to the localized plastic deformation. This point was further verified by comparing the morphology of worn surfaces in these two samples shown by SEM images in Figs. 11(a) and (b), respectively. Micrographs revealed that dominant wear mechanism in the Al5083 base metal sample is severe adhesive with a lot of surface damage and smearing. The variation of the friction coefficient in Fig. 10(a) also signifies the evidence of intensive plastic deformation and material removal in this sample.

As the sliding continues, loose wear particles form, deform, fracture, and lead to the formation of smaller debris. Wear debris may act as abrasives and scratch the surface as a series of grooves parallel to the sliding direction. This is the case with the FSPed base metal (Fig. 11(b)) where both the adhesive and abrasive wear signs (in the form of shallow wear grooves) are evident on the worn surface. In the FSPed base metal, the plastic deformation and the adhesive wear are less than the un-FSPed base metal. This fact can even be noticed while comparing the wear debris in these two specimens. The wear debris of the base metal (Fig. 12(a)) exhibited irregular plate-like morphology and were larger in size as compared to that of the FSPed base metal (Fig. 12(b)), and was in agreement with the results of their wear volume loss and wear rates.

As stated earlier, significant improvement in wear resistance of SMMCs is attained (Figs. 8 and 9). It is basically attributed to the surface hardening mechanisms resulted from the addition of reinforcement particles and

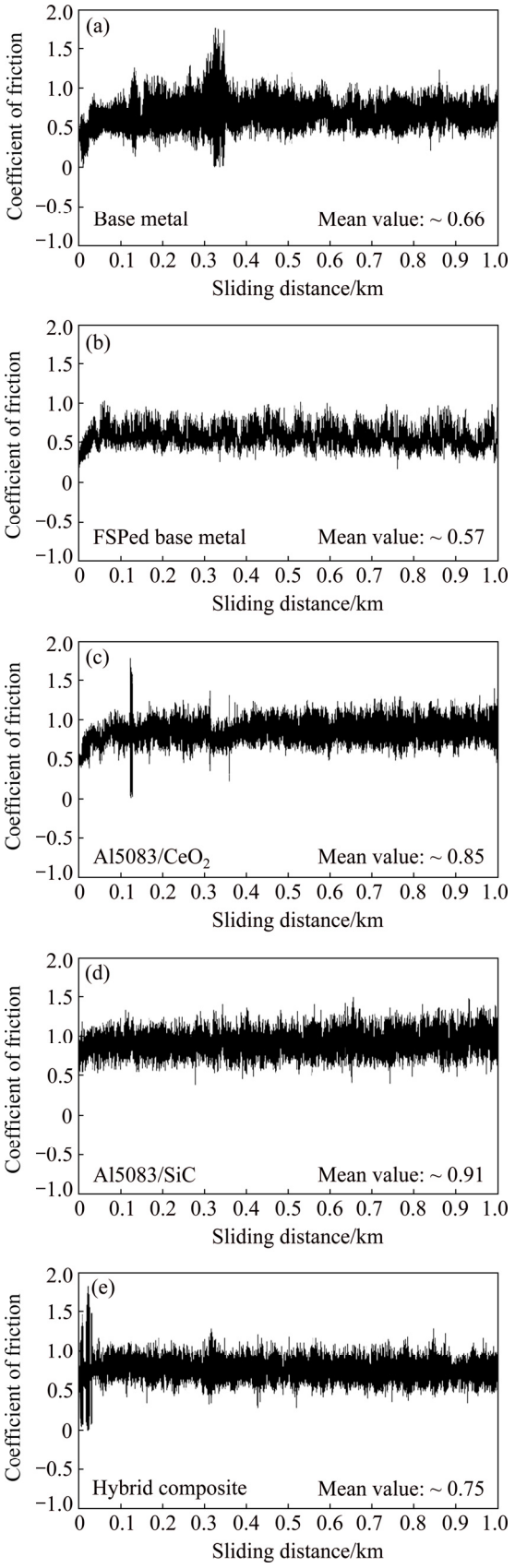

Fig. 10 Variation of coefficient of friction with sliding distance for Al5083 base metal and FSPed specimens (In each case the mean value of friction coefficient is also determined for comparison purpose)

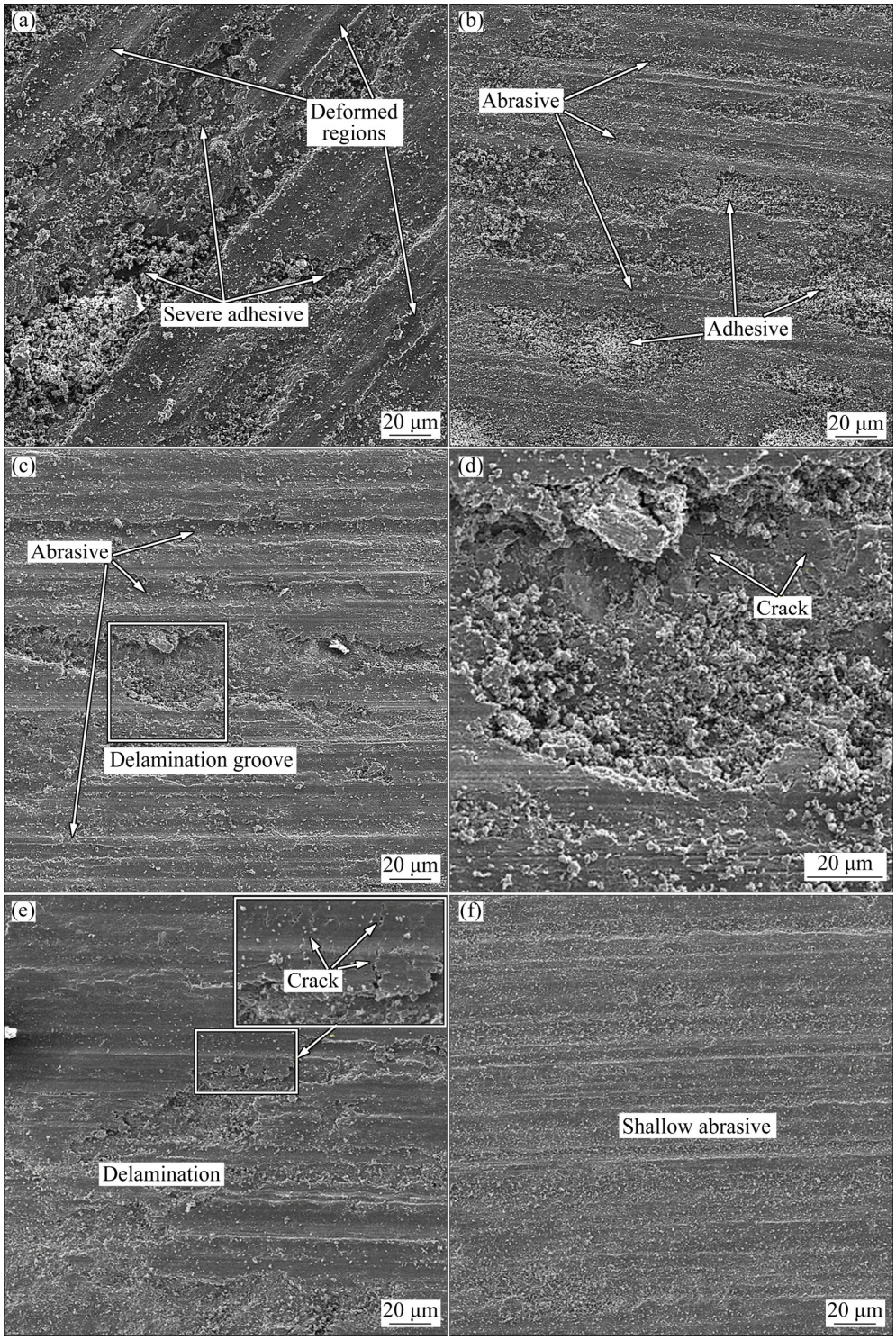

Fig. 11 SEM images of worn surfaces after 1 km sliding of different samples: (a) Base metal; (b) FSPed base metal; (c) Al5083/CeO_2; (d) Higher magnification of Fig. (c) marked by white rectangle indicating subsurface microcracking and delamination wear; (e) Al5083/SiC with severe surface cracks and delamination; (f) Al5083/CeO_2/SiC hybrid composite with less surface damage and shallow abrasive grooves

microstructural modification induced by the FSP leading to higher hardness. It is also agreed that the hard reinforcement particles either individually or in the combined form, bear the applied loads and impede direct load contact of aluminum matrix (pin) and counterface (disk) [11,40,41]. So, it is expected in the presence of higher number of SiC and/or CeO_2 particles in nanocomposite layer, wear resistance increased. It is true in particular with the hybrid SMMC exhibiting the best wear resistance among all the wear tested specimens.

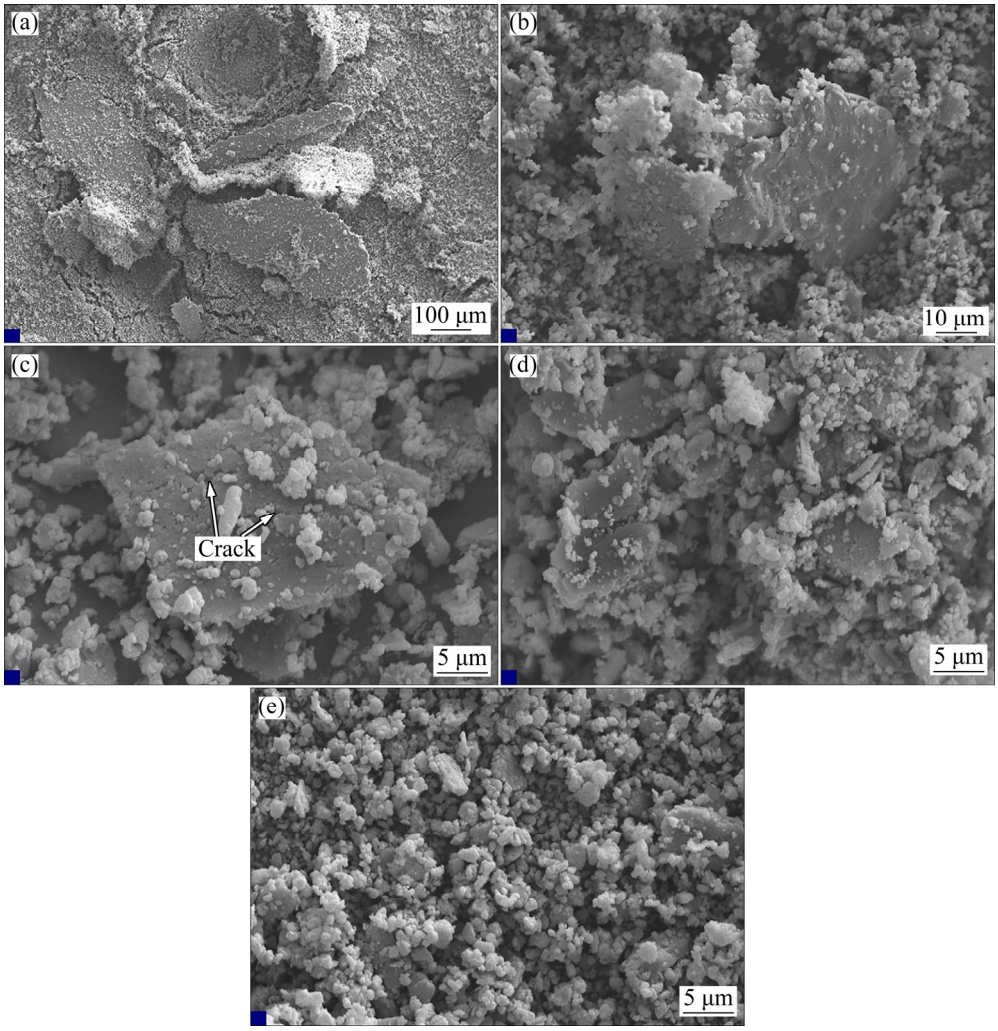

Fig. 12 SEM images of wear debris for different wear tested specimens: (a) Base metal; (b) FSPed base metal; (c) Al5083/CeO_2; (d) Al5083/SiC; (e) Al5083/CeO_2/SiC hybrid composite

Abrasive wear and delamination were found to be the dominant wear mechanisms in specimens with surface composite layer because hard reinforcing SiC and CeO_2 particles prevent adhesive wearing and extensive deformation and materials removal. In the case of the Al5083/CeO_2 mono composite, the micrograph of worn surface (Fig. 11(c)) reveals shallow depths and narrow abrasive grooves.

Delamination wear (abrasive wear aided) was also noticed in this sample (Fig. 11(d)) covered with fine wear debris. This wear mechanism was identified by observation of cracks under wear tracks. In this mechanism, thin lamellar wear debris in the form of flakes is formed and removed from the surface due to the nucleation and propagation of subsurface cracks. In fact, initial voids are nucleated around the reinforcing particles or second phase particles, leading to crack initiation [42]. The delamination wear mechanism was more apparent in the Al5083/SiC mono composite layer, as shown in Fig. 11(e).

In the present work, worn surface of hybrid SMMC was smoother with a fewer shallow grooves (Fig. 11(f)) as compared to mono SMMCs. Hybrid SMMC also exhibited the lowest mean friction coefficient among SMMCs as shown in Fig. 10. The mean coefficients of friction were ~0.75, ~0.85 and ~0.91 for hybrid SMMC, Al5083/CeO_2 and Al5083/SiC, respectively. In fact, the enhancement in wear resistance, and the low friction coefficient of hybrid SMMC are attributed to the solid lubrication effect provided by CeO_2 particles. Many investigators have reported superior wear resistance of hybrid composites to that of mono composites [9−17]. They have stated that solid lubricant effect caused by one of the reinforcements enhanced the wear resistance of hybrid composite. In all these investigations, the softer reinforcement has acted and played the role of a solid lubricant in the composite. In the present study, CeO_2 particles act as an effective solid lubricant since they are

softer than SiC particles. It is expected that during sliding CeO_2 particles are pulled out and a thin tribo layer is formed. The repeated formation of this layer at the interface reduces the friction between the steel counterface and the sliding composite surface. In other words, CeO_2 particles have the role of self-lubricating in this case. This effect can clearly be noticed and verified while comparing the wear resistance and friction coefficient of the Al5083/SiC mono composite and hybrid SMMC. In the former case, no lubricating layer could be formed and thereby friction coefficient reached the maximum, where delamination wear is dominated. The worn surface morphology in Fig. 11 specifies that a clear deformed layer is formed in the case of Al5083/CeO_2 composite (Fig. 11(c)). Furthermore, a minimum coefficient of friction in combination with a high hardness reduced the extent of wear in surface composite reinforced with SiC and CeO_2 particles. The morphologies of wear debris for the Al5083/CeO_2 and the Al5083/SiC mono composites are shown in Figs. 12(c) and (d), respectively. In these mono composites, wear flakes are distinctive from the hybrid SMMC where wear debris is considerably fine and flake size is remarkably smaller due to the lubricating effect of CeO_2 particles. This is shown in Fig. 12(e) for the hybrid SMMC. Thus, it can be concluded that the dominant wear mechanism in the FSPed and un-FSPed base alloy is severe adhesive, which further changes to shallow abrasive and delamination in mono Al5083/(SiC and CeO_2) surface layer composites. The shallow abrasive wear mechanism was also identified for Al5083/CeO_2/SiC hybrid composite layer with the best wear performance.

4 Conclusions

1) The FSP led to uniform distribution of reinforcements in the NZ and refined the grains significantly. No defects were observed at the interface as well as in the processed zone. Increasing the number of passes and also changing the processing directions, led to a more homogeneous NZ and better distribution of reinforcements with fine grains.

2) All the composite samples showed higher hardness and wear resistance compared to the base metal and the FSPed base metal with no reinforcement. The best wear performance was obtained for the Al5083/CeO_2/SiC hybrid composite.

3) The enhancement in wear resistance and the lowest friction coefficient of the hybrid composites are attributed to the solid lubrication effect provided by CeO_2 particles.

4) During sliding wear test, reinforcing particles SiC and CeO_2 altered the morphology of wear debris and wear mechanism. The wear mode is transformed from severe adhesive in the un-FSPed and the FSPed base alloy to shallow abrasive wear and delamination in specimens with mono composite layers, whereas hybrid composite showed merely shallow abrasive wear mechanism. Morphologies of the wear debris and flakes also changed in the similar manner from larger and irregular ones to much finer and smaller ones in mono and hybrid composite layers, respectively.

Acknowledgment

The authors highly appreciate the financial support provided by Shahid Chamran University of Ahvaz, Iran.

References

[1] MIRACLE D B. Metal matrix composites–From science to technological significance [J]. Composites Science and Technology, 2005, 65(15): 2526−2540.

[2] ATTIA A N. Surface metal matrix composites [J]. Materials & Design, 2001, 22(6): 451−457.

[3] WANG Y, ZHANG X, ZENG G, LI F. In situ production of Fe−VC and Fe−TiC surface composites by cast-sintering [J]. Composites: Part A, 2001, 32(2): 281−286.

[4] LEE J, EUH K, OH J C, LEE S. Microstructure and hardness improvement of TiC/stainless steel surface composites fabricated by high-energy electron beam irradiation [J]. Materials Science and Engineering A, 2002, 323(1): 251−259.

[5] CULHA O, TEKMEN C, TOPARLI M, TSUNEKAWA Y. Mechanical properties of in situ Al_2O_3 formed Al−Si composite coating via atmospheric plasma spraying [J]. Materials & Design, 2010, 31(1): 533−544.

[6] VEREZUB O, KALAZI Z, SYTCHEVA A, KUZSELLA L, BUZA G, VEREZUB N V, FEDOROV A, KAPTAY G. Performance of a cutting tool made of steel matrix surface nano-composite produced by in situ laser melt injection technology [J]. Journal of Materials Processing Technology, 2011, 211(4): 750−758.

[7] MA Z Y. Friction stir processing technology: A review [J]. Metallurgical and Materials Transactions A, 2008, 39(3): 642−658.

[8] MISHRA R S, MA Z Y, CHARIT I. Friction stir processing: A novel technique for fabrication of surface composite [J]. Materials Science and Engineering A, 2003, 341(1): 307−310.

[9] SOLEYMANI S, ABDOLLAH-ZADEH A, ALIDOKHT S A. Microstructural and tribological properties of Al5083 based surface hybrid composite produced by friction stir processing [J]. Wear, 2012, 278−279: 41−47.

[10] MOSTAFAPOUR-ASL A, KHANDANI S T. Role of hybrid ratio in microstructural, mechanical and sliding wear properties of the Al5083/graphite$_p$/Al_2O_{3p} surface hybrid nanocomposite fabricated via friction stir processing method [J]. Materials Science and Engineering A, 2013, 559(2): 549−557.

[11] MAHMOUD-ESSAM R I, TAKAHASHI M, SHIBAYANAGI T, IKEUCHI K. Wear characteristics of surface−hybrid−MMCs layer fabricated on aluminum plate by friction stir processing [J]. Wear, 2010, 268(9): 1111−1121.

[12] MAXWELL-REJIL C, DINAHARANB I, VIJAYB S J, MURUGANC N. Microstructure and sliding wear behaviour of AA6360/(TiC+B_4C) hybrid surface composite layer synthesized by friction stir processing on aluminum substrate [J]. Materials Science and Engineering A, 2012, 552: 336−344.

[13] YUVARAJ N, ARAVINDAN S, VIPIN. Wear characteristics of Al5083 surface hybrid nano-composites by friction stir processing [J]. Transactions of the Indian Institute of Metals, 2016, 70(4): 1111−1129.

[14] PALANIVEL R, DINAHARAN I, LAUBSCHER R F, PAULO DAVIM J. Influence of boron nitride nanoparticles on microstructure and wear behavior of AA6082/TiB_2 hybrid aluminum composites synthesized by friction stir processing [J]. Materials & Design, 2016, 106(1): 195−204.

[15] ARURI D, ADEPU K, ADEPU K, BAZAVAD K. Wear and mechanical properties of 6061-T6 aluminum alloy surface hybrid composites ((SiC+Gr) and (SiC+Al_2O_3)) fabricated by friction stir processing [J]. Journal of Materials Research and Technology, 2013, 2(4): 362−369.

[16] BARENJI R V, KHOJASTEHNEZHAD V M, POURASL H H, RABIEZADEH A. Wear properties of Al−Al_2O_3/TiB_2 surface hybrid composite layer prepared by friction stir process [J]. Journal of Composite Materials, 2016, 50(11): 1457−1466.

[17] ALIDOKHT S A, ABDOLLAH-ZADEH A, SOLEYMANI S, ASSADI H. Microstructure and tribological performance of an aluminium alloy based hybrid composite produced by friction stir processing [J]. Materials & Design, 2011, 32(5): 2727−2733.

[18] MISHRA R S, MA Z Y. Friction stir welding and processing [J]. Materials Science and Engineering R, 2005, 50(1): 1−78.

[19] GANDRA J, MIRANDA R, VILAC P, VELHINHO A, TEIXEIRA J P. Functionally graded materials produced by friction stir processing [J]. Journal of Materials Processing Technology, 2011, 211(11): 1659−1668.

[20] BATZILL M, DIEBOLD U. Surface studies of gas sensing metal oxides [J]. Physical Chemistry Chemical Physics, 2007, 9(19): 2307−2318.

[21] ASHRAF P M, SHIBLI S M A. Reinforcing aluminium with cerium oxide: A new and effective technique to prevent corrosion in marine environments [J]. Electrochemistry Communications, 2007, 9(3): 443−448.

[22] YANG L, PANG X, FOX-RABINOVICH G, VELDHUIS S, ZHITOMIRSKY I. Electrodeposition of cerium oxide films and composites [J]. Surface and Coatings Technology, 2011, 206(1): 1−7.

[23] AMRA M, RANJBAR K, DEHMOLAEI R. Mechanical properties and corrosion behavior of CeO_2 and SiC incorporated Al5083 alloy surface composites [J]. Journal of Materials Engineering and Performance, 2015, 24(8): 3169−3179.

[24] SU J Q, NELSON T W, STERLING C J. Microstructure evolution during FSW/FSP of high strength aluminum alloys [J]. Materials Science and Engineering A, 2005, 405(1): 277−286.

[25] MCNELLEY T R, SWAMINATHAN S, SU J Q. Recrystallization mechanisms during friction stir welding/processing of aluminum alloys [J]. Scripta Materialia, 2008, 58(5): 349−354.

[26] SATO Y S, PARK S H C, KOKAWA H. microstructural factors governing hardness in friction-stir welds of solid-solution-hardened Al alloys [J]. Metallurgical and Materials Transactions A, 2001, 32(12): 3033−3042.

[27] JOHANNES L B, CHARIT I, MISHRA R S, VERMA R. Enhanced superplasticity through friction stir processing in continuous cast AA5083 aluminum [J]. Materials Science and Engineering A, 2007, 464(1): 351−357.

[28] GARCIA BERNAL M A, MISHRA R S, VERMA R, HERNANDEZ SILVA D. Hot deformation behavior of friction-stir processed strip-cast 5083 aluminum alloys with different Mn contents [J]. Materials Science and Engineering A, 2012, 534(1): 186−192.

[29] KRISHNAN K N. On the formation of onion rings in friction stir welds [J]. Materials Science and Engineering A, 2002, 327(2): 246−251.

[30] MORISADA Y, FUJII H, NAGAOKA T, NOGI K, FUKUSUMI M. Fullerene/A5083 composites fabricated by material flow during friction stir processing [J]. Composites: Part A, 2007, 38(10): 2097−2101.

[31] ASADI P, BESHARATI-GIVI M K, ABRINIA K, TAHERISHARGH M, SALEKROSTAM R. Effects of SiC particle size and process parameters on the microstructure and hardness of AZ91/SiC composite layer fabricated by FSP [J]. Journal of Materials Engineering and Performance, 2011, 20(9): 1554−1562.

[32] LIU Q, KE L, LIU F, HUANG C, XING L. Microstructure and mechanical property of multi-walled carbon nanotubes reinforced aluminum matrix composites fabricated by friction stir processing [J]. Materials & Design, 2013, 45: 343−348.

[33] RUFF A W. ASM handbook on friction, lubrication, and wear technology: Introduction to laboratory characterization techniques [M]. Ohio, USA: ASM International, 1992: 629−742.

[34] HUANG K T, LUI T S, CHEN L H. Effect of microstructural feature on the tensile properties and vibration fracture resistance of friction stirred 5083 alloy [J]. Journal of Alloys and Compounds, 2011, 509(27): 7466−7472.

[35] CUI G R, MA Z Y, LI S X. The origin of non-uniform microstructure and its effects on the mechanical properties of a friction stir processed Al−Mg alloy [J]. Acta Materialia, 2009, 57(19): 5718−5729.

[36] ZHANG Z, CHEN D L. Contribution of Orowan strengthening effect in particulate-reinforced metal matrix nanocomposites [J]. Materials Science and Engineering A, 2008, 483−484(1): 148−152.

[37] HUQ M Z, CELIS J P. Reproducibility of friction and wear results in ball-on-disc unidirectional sliding tests of TiN−alumina pairings [J]. Wear, 1997, 212(2): 151−159.

[38] MAJUMDAR J D, CHANDRA B R, MANNA I. Friction and wear behavior of laser composite surfaced aluminium with silicon carbide [J]. Wear, 2007, 262(5): 641−648.

[39] UYYURU R K, SURAPPA M K, BRUSETHAUG S. Tribological behavior of Al−Si−SiC_p composites/automobile brake pad system under dry sliding conditions [J]. Tribology International, 2007, 40: 365−373.

[40] DOLATKHAH A, GOLBABAEI P, BESHARATI-GIVI M K, MOLAIEKIYA F. Investigating effects of process parameters on microstructural and mechanical properties of Al5052/SiC metal matrix composite fabricated via friction stir processing [J]. Materials & Design, 2012, 37(2): 458−464.

[41] SHYAM KUMAR C N, BAURI R, YADAV D. Wear properties of 5083 Al−W surface composite fabricated by friction stir processing [J]. Tribology International, 2016, 101: 284−290.

[42] SUH N P. The delamination theory of wear [J]. Wear, 1973, 25(1): 111−124.

搅拌摩擦加工制备具有单一和混合表面的 Al5083/CeO_2/SiC 复合材料的显微组织和磨损行为

M. AMRA, Khalil RANJBAR, S. A. HOSSEINI

Department of Materials Science and Engineering, Faculty of Engineering,
Shahid Chamran University of Ahvaz, Ahvaz 61357, Iran

摘　要：利用搅拌摩擦加工(FSP)，将纳米尺寸的氧化铈(CeO_2)和碳化硅(SiC)颗粒以单独和混合形式嵌入 Al5083 合金基体，制备表面复合材料，并研究这些增强相对合成的表面复合层显微组织和耐磨性能的作用。在室温下用销−盘式磨损试验机检测合成的单独和混合表面复合层的磨损特性。用光学显微镜和扫描电镜观察 FSPed 区和磨损表面的显微组织。在熔核区可观察到显著的晶粒细化和均匀分布的增强颗粒。与基体金属相比，所有复合材料都具有更高的硬度和更好的耐磨性。其中，混合复合材料 Al5083/CeO_2/SiC 的耐磨性能最好，摩擦因数最低，而 Al5083/SiC 的硬度最高，是 Al5083 基体合金硬度的 1.5 倍。混合复合材料表面耐磨性能的提高是由于 CeO_2 颗粒的固体润滑效果。非复合材料中主要的磨损机制是严重的粘着磨损，当存在增强颗粒时转变为磨粒磨损和分层。

关键词：Al5083 合金；搅拌摩擦加工；CeO_2；SiC；表面复合材料；磨损机制

(Edited by Wei-ping CHEN)